IEEE Photonics Journal
An IEEE Photonics Society Publication

Open Access

Coherent Radio-Over-Fiber and Millimeter-Wave Radio Seamless Transmission System for Resilient Access Networks

Volume 4, Number 6, December 2012

A. Kanno, Member, IEEE
P. T. Dat, Member, IEEE
T. Kuri, Member, IEEE
I. Hosako, Member, IEEE
T. Kawanishi, Member, IEEE
Y. Yoshida, Member, IEEE
Y. Yasumura
K. Kitayama, Fellow, IEEE

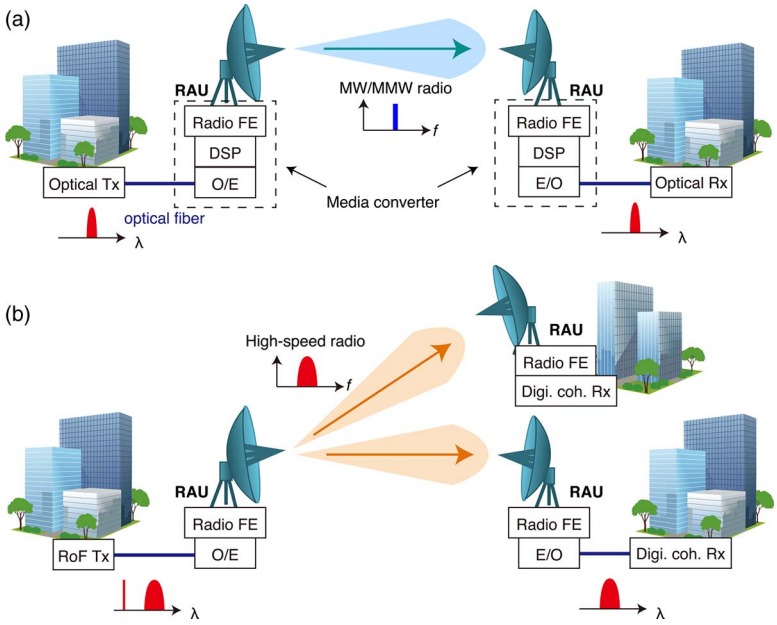

DOI: 10.1109/JPHOT.2012.2228182
1943-0655/$31.00 ©2012 IEEE

IEEE photonics SOCIETY

IEEE

Coherent Radio-Over-Fiber and Millimeter-Wave Radio Seamless Transmission System for Resilient Access Networks

A. Kanno,[1] *Member, IEEE*, P. T. Dat,[1] *Member, IEEE*, T. Kuri,[1] *Member, IEEE*, I. Hosako,[2] *Member, IEEE*, T. Kawanishi,[1] *Member, IEEE*, Y. Yoshida,[3] *Member, IEEE*, Y. Yasumura,[3] and K. Kitayama,[3] *Fellow, IEEE*

[1]Photonic Network Research Institute, National Institute of Information and Communications Technology, Tokyo 184-8795, Japan
[2]Advanced ICT Research Institute, National Institute of Information and Communications Technology, Tokyo 184-8795, Japan
[3]Graduate School of Engineering, Osaka University, Osaka 565-0871, Japan

DOI: 10.1109/JPHOT.2012.2228182

Manuscript received September 21, 2012; revised November 5, 2012; accepted November 9, 2012. Date of publication November 20, 2012; date of current version December 3, 2012. Y. Yasumura, Y. Yoshida, and K. Kitayama are thankful for the financial support received from the "Agile deployment capability of highly resilient optical and radio seamless communication systems" program of the commissioned research of the National Institute of Information and Communications Technology (NICT).
Corresponding author: A. Kanno (e-mail: kanno@nict.go.jp).

Abstract: We propose a millimeter-wave (MMW) coherent radio-over-fiber (RoF) transmission system for application to an access network with a direct broadband last-mile wireless connection to an optical fiber network. The coherent RoF system comprises an optical two-tone RoF signal generator with an advanced modulation format for high-throughput transmission and employs a digital-signal-processing-aided coherent detection technique for MMW radio, which is a technique similar to that of optical digital coherent detection. As proof of concept, a 20-GBd quadrature phase-shift keying RoF transmission over 20 km of optical fiber before a radio transmission over 20 m of air is demonstrated. The results of the radio transmissions using Cassegrain-type antenna pairs with a gain of 50 dBi are consistent with theoretical estimations; this suggests the possibility of developing a midrange transmission system using a high-power MMW amplifier.

Index Terms: Radio-over-fiber (RoF), coherent detection, millimeter-wave (MMW).

1. Introduction

Direct conversion between wired (optical) and wireless (radio) networks is an emerging issue in the enhancement of network resilience against a disaster, as well as in last-mile access networks including mobile backhauling for future mobile communications. In particular, during the Great East Japan Earthquake, which occurred on March 11, 2011, a large number of optical fiber cables were severed, and as a result, almost all broadband links, including the mobile backhaul, were disconnected [1], [2]. Thus, complete restoration of the optical fiber network is expected to require one to two years. However, the quick deployment of broadband connections immediately after a disaster has been strongly desired for rescue and surveillance [3]. In addition, a high-capacity connection has also been desired for the remote surveillance of important facilities such as nuclear power plants. To immediately provide a broadband connection, a high-speed radio connection is a

possible candidate; however, conventional and commercially available radio communication standards are not suitable because of their poor capacity of 1 Gb/s, which is insufficient for the Long Term Evolution (LTE)-Advanced standard for cellular communications and the IEEE 802.11ac standard for wireless local area networks [4], [5]. This poor capacity is caused by a limitation on the available bandwidth in the microwave (MW) region.

Millimeter-wave (MMW) radio with radio-over-fiber (RoF) technology is one possible candidate for providing and delivering high-speed radio transmission with a capacity greater than 10 Gb/s [6]–[9]. The direct photonic upconversion technique can provide seamless media conversion from an RoF signal, which consists of optical baseband and reference components, to an MMW signal [10]. In addition, the recent development of an optical coherent detection technique involving the use of high-speed digital signal processing (DSP) is helping in the achievement of higher spectral efficiency in optical signals using a multilevel modulation technique. Consequently, it would be natural to apply high-speed electronics such as an analog-to-digital converter (ADC) and an algorithm for demodulation to MMW radio detection. Moreover, transmission impairments, including the frequency response of the transmitter (Tx) and receiver (Rx), would be compensated by DSP at a digital coherent Rx; that is, no DSP would be required at repeating points.

In this paper, we present an MMW coherent RoF and radio transmission system for seamless optical-radio transmission. As proof of concept, a high-speed radio transmission over 20 m of free space after an optical transmission over a 20-km fiber without any DSP at the radio access units (RAUs) is demonstrated. A coherent optical two-tone generator, which is based on an optical modulation technique, provides an MMW RoF signal with high-frequency stability for easy demodulation and compliance with radio regulations. A high-gain antenna can extend the transmission distance and make the system applicable to access networks such as those employing a last-mile solution.

2. Coherent RoF and Seamless Radio Transmission for an Access Network

Fig. 1 shows schematic illustrations of the conventional and proposed optical-radio-optical transmission systems. In the conventional design, the system comprises an optical Tx, RAUs that are connected to optical fibers, and an optical Rx [see Fig. 1(a)]. The optical Tx transmits a baseband optical signal over the optical fiber connected to an RAU. The DSP at the RAU performs deserialization and signal optimization for radio transmission to demodulate the original payload after the optical-to-electrical (O/E) conversion of the received optical signal in order to generate the desired radio signal with an appropriate modulation format for the DSP. Then, a radio front-end (FE) that consists of amplifiers transmits the radio signal over the air through an antenna. In conventional fixed wireless access (FWA) transmission, the carrier frequency of the radio signal ranges from the MW region to the MMW region, which is typically a 25-GHz band for a building-to-building connection. In 25-GHz-band FWA communication, the available bandwidth for radio communications is considerably smaller than 1 GHz, and thus, the signal form is based on higher-order multilevel modulation to optimize the throughput. The receiver-side RAU detects the radio signal at a radio FE. Compensation of transmission impairments such as a fading effect is performed before carrying out media conversion by serializing at another DSP. The data are detected from the radio signal converted from an optical signal with an electrical-to-optical (E/O) conversion, and the optical signal is transmitted over another optical fiber. In this situation, the total throughput can be limited by the processing capability of the DSP because the modulation speed is significantly higher than the processing speed of the DSP. Moreover, such a highly functioning DSP would increase the energy consumption of the RAU. Therefore, a reduction in the number of DSPs would improve the total performance of the transmission system.

Fig. 1(b) shows the proposed concept of the optical-radio-optical transmission system based on RoF and DSP-aided coherent detection technologies. To reduce the number of DSPs, the system is comprised of two key components: an RoF Tx and a digital coherent Rx. The RoF signal, which consists of an optical baseband component similar to a conventional optical signal and an optical reference component working as an optical local oscillator (LO) signal, is formed and transmitted

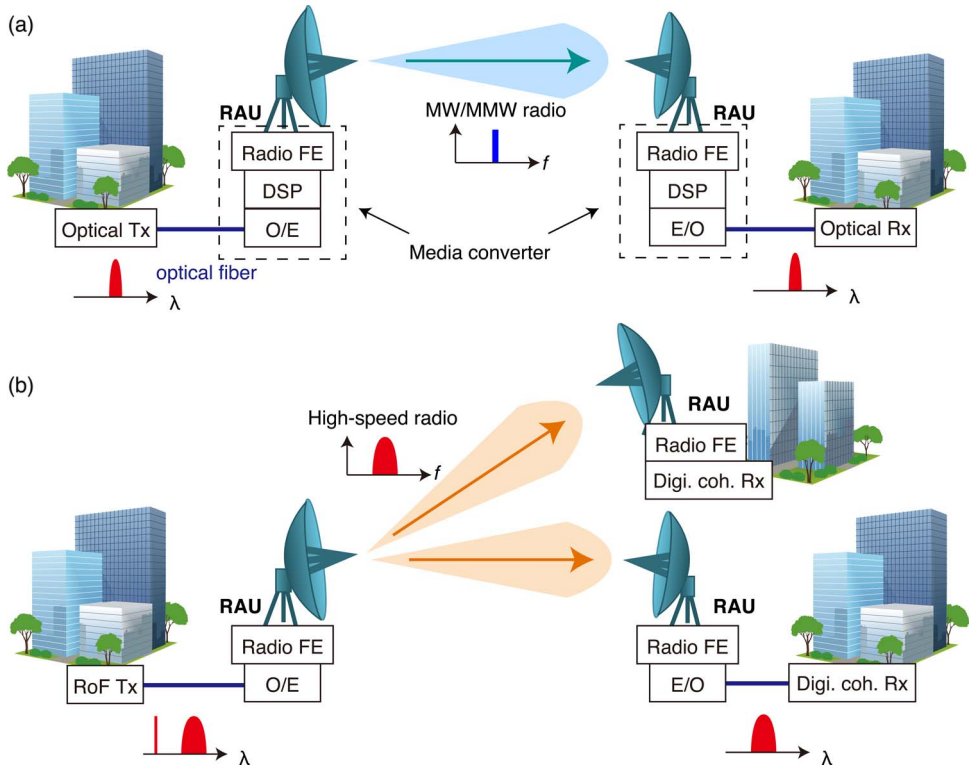

Fig. 1. Schematic illustrations of the configuration for (a) the conventional FWA link and (b) the proposed MMW RoF link. The coarse spectra for optical and radio transmissions are also shown.

over the fiber from the RoF Tx. At the RAU, the RoF signal is converted into a radio signal with a direct photonic conversion technique at an O/E converter, and then, a directly connected radio FE irradiates the formed radio signal with no DSP unit. At the receiver RAU, the received radio signal is also directly converted into an optical signal using a high-speed optical modulator [11]. The digital coherent Rx can demodulate the optical signal with impairment compensation for the entire transmission system, including the optical and radio components. Recent digital coherent receivers include dispersion compensation for optical fiber transmission, a certain function for frequency-domain equalization, and phase noise suppression of the transmitted signals. Particularly in 100-Gb/s-class optical transport networks, signal compensation technology for the modulation format of a dual-polarization quadrature phase-shift keying (DP-QPSK) transmission should be implemented with an adaptive equalization technique such as a constant-modulus algorithm; this is also available for radio transmission. Therefore, transmission impairment compensation can be performed. For the realization of simple radio transmission such as a last-mile solution from the RAU to a home or an office that is similar to an FWA transmission, the RAU can be configured with a radio FE and a digital coherent Rx for radio transmission [12]. We discuss this optical-radio transmission system in the feasibility study for the proof of concept, presented in the next section.

For applications on an access network, the achievable transmission distance is one of the most important factors for a radio transmission system. In the MMW region, atmospheric attenuation plays an important role in transmission because the attenuation coefficient is significantly larger in the MMW region than in the MW region, which is typically 15 dB/km in the 60-GHz band and 0.5 dB/km in the 90-GHz band. Thus, a high-power radio amplifier or a high-gain antenna is required to extend the transmission distance. A quasi-optic configuration, such as a parabolic antenna or an antenna with a Cassegrain-type reflector, is applicable as a high-gain antenna because its antenna gain depends not on the material but on the design. Although broadband amplifiers with high linearity and high output power have been developed in several studies, it is presently not easy to apply these

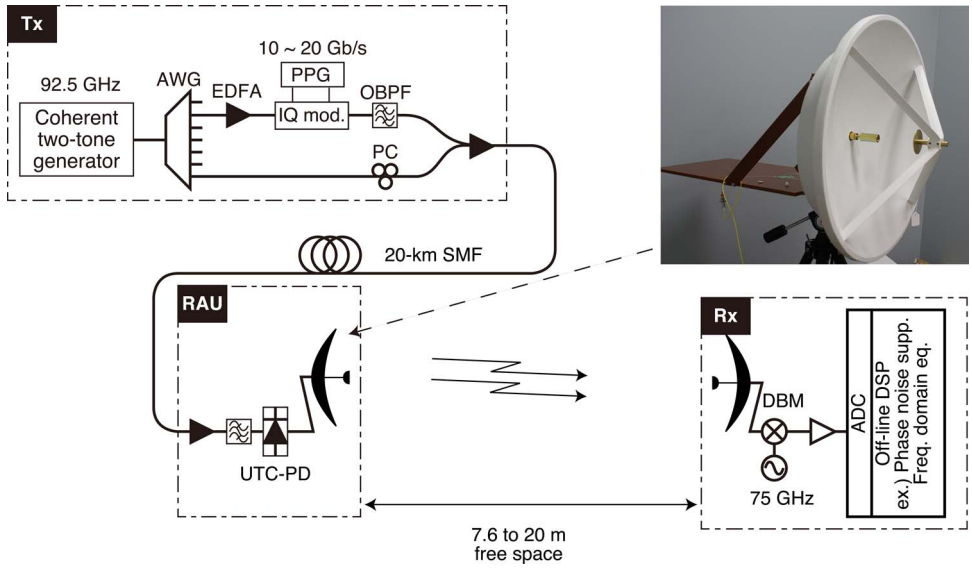

Fig. 2. Experimental setup.

amplifiers [13], [14]. Herein, we attempt to extend the transmission distance and evaluate the feasibility of the proposed system using a high-gain antenna.

3. Experimental Details

3.1. Experimental Setup

The experimental setup for seamless conversion from an optical signal to an MMW radio signal with high-gain antennas is shown in Fig. 2 [15]. At the RoF Tx, a coherent optical two-tone generator operated at 23.125 GHz, corresponding to a quarter of the MMW RoF frequency, generates a 92.5-GHz-separated optical two-tone signal. The details of the coherent two-tone generator are given in the next subsection. The optical two-tone signal was split into an upper sideband (USB) component and a lower sideband (LSB) component by an arrayed waveguide grating (AWG). The USB component of the optical signal was modulated by an optical inphase/quadrature (IQ) modulator connected to a two-channel pulse pattern generator (PPG) after it had passed through an erbium-doped fiber amplifier (EDFA). The symbol pattern was a pseudorandom bit sequence with a length of $2^{15} - 1$ bits. An optical bandpass filter (OBPF) reshaped the QPSK-modulated signal in order to reduce undesired sidelobe components. The LSB component was utilized as an optical reference component, that is, an optical LO component, and then, the state of polarization of the LSB was optimized by a polarization controller (PC). The combined USB and LSB components, which formed an RoF signal, were amplified by the EDFA and then fed into a 20-km-long single-mode fiber (SMF) for optical transmission. At the RAU, the transmitted RoF signal was amplified again by the EDFA placed before the OBPF to reduce the amplified spontaneous emission noise. A unitraveling carrier photodiode (UTC-PD), which was utilized as a photomixer, directly converted the RoF signal into the MMW radio signal. A Cassegrain-type antenna with an antenna gain of 50 dB, which is shown in the inset in Fig. 2, was directly connected to the UTC-PD with a standard waveguide, and it irradiated the radio signal over the air. The transmission distance was 7.6–20 m in a large-scale anechoic chamber. At the Rx, the antenna, which was identical to the antenna at the RAU, received the radio signal and then fed it into a heterodyning detector, which was comprised of a double-balanced mixer (DBM) connected to an electrical LO operating at 75 GHz. This MMW LO was consisted with a harmonic multiplier with a multiplication number of 5 and a free-running MW synthesizer. A downconverted intermediate frequency (IF) component was captured by an ADC, which functioned as a real-time oscilloscope in this experiment. The analog bandwidth and sampling

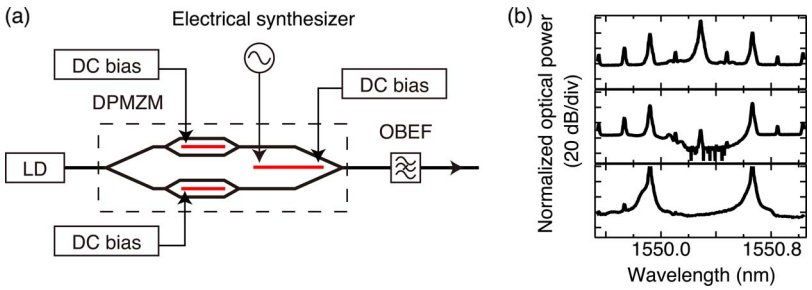

Fig. 3. (a) Configuration of the coherent optical two-tone generator and (b) the optical spectrum of the 92.5-GHz-separated optical two-tone signal observed at an output port of the modulator (top), the output of the OBEF (middle), and the resultant two-tone signal after the AWG (bottom).

rate of the ADC were 30 GHz and 80 GSa/s, respectively. The digitized signal was processed by an offline DSP for demodulation and analysis; the DSP was configured to perform a conventional optical digital coherent detection technique without carrier frequency offset compensation. The DSP used digital IQ separation, phase noise suppression, downsampling, frequency-domain equalization, and a bit-error-rate (BER) test [8].

3.2. Coherent Optical Two-Tone Generation Based on Optical Modulation

The configuration of the coherent optical two-tone generator is shown in Fig. 3(a) [16]. A continuous-wave optical signal emitted from a laser diode (LD) was fed into a dual-parallel Mach–Zehnder interferometer modulator (DPMZM), having a structure similar to that of an optical IQ modulator. This DPMZM was used to realize a high extinction ratio when the nested MZMs were driven by a dc voltage, for the compensation of the optical intensity imbalance due to a fabrication error in the Y-branch of the main MZM [17]. These nested MZMs were employed as intensity trimmers in each arm, to ensure that the optical intensity difference between the two arms in the main MZM would be compensated. An electrical signal fed to an electrode of the main MZM could cause the generation of sideband components. Essentially, only even-order components were generated when the bias voltage of the main MZM was set at the maximum transmission point. However, the degradation of the extinction ratio of the modulator led to incomplete suppression of the odd-order components. Thus, a high extinction ratio is indispensable for clear optical two-tone generation. The modulated optical signal was passed through an optical band elimination filter (OBEF) for the suppression of the carrier component. Finally, only the second-order components were generated, that is, optical two-tone generation with a frequency separation of a quadruple frequency of the fed electrical signal was achieved. Fig. 3(b) shows the optical spectrum of a generated two-tone signal with a separation of 92.5 GHz, which corresponds to the fed electrical frequency of 23.125 GHz. A side-mode suppression ratio (SMSR) of more than 40 dB was achieved for the first-order components of the modulated signals [top panel in Fig. 3(b)]. Residual third-order components might have been caused by an imbalance of the amplitude of the electrical signal fed into the modulator in each arm of the main MZM. Undesired components were suppressed by the AWG, and thus, an SMSR of about 20 dB for third-order components would be insignificant in the resultant optical signal quality.

The phase noise of the generated two-tone signal plays an important role in coherent RoF transmission because an advanced modulation format such as QPSK requires a low-phase-noise carrier. There are some reports on the phase noise analysis for the optical two-tone signal generated by this method [18], [19]. Theoretically, the phase noise degradation provided by a multiplication is expressed by $20\log m$, where m is the multiplication factor; the observed phase noise behavior follows this equation. In addition, the phase noise and frequency were well stabilized because only one electrical synthesizer generated the transmitted electrical signal. Essentially, an electrical multiplier degrades the phase noise more than the theoretical estimated value. Thus, the optical multiplication method utilized by the two-tone generation would have an advantage not only in terms of both the phase noise and frequency stabilization.

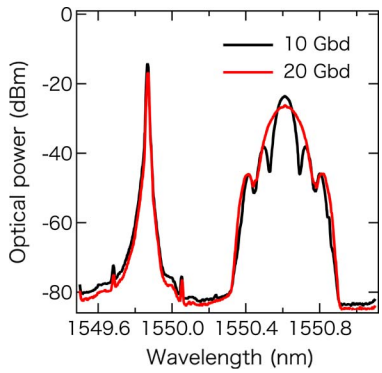

Fig. 4. Optical spectra of RoF signals for 10-GBd (black) and 20-GBd (red) transmissions observed at the input port of the UTC-PD.

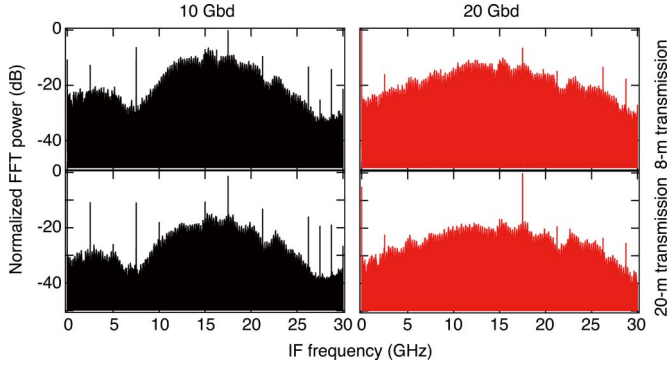

Fig. 5. FFT power spectra of received IF component for 10-GBd (black) and 20-GBd (red) signals under transmission distances of 8 m (top) and 20 m (bottom).

4. Results

Fig. 4 shows the optical spectra for the 10-GBd and 20-GBd QPSK RoF signals observed at the input port of the UTC-PD. A clear separation of 92.5 GHz, which corresponds to approximately 0.74 nm, is observed for an SMSR above 40 dB. The observed distortion of the sidelobe components for the 20-GBd signal was caused by the OBPF placed at the output of the optical IQ modulator for reducing the number of undesired components. The fast Fourier transform (FFT) spectra of the received IF signals at the Rx are shown in Fig. 5. A DBM fed from the electrical LO signal at the frequency of 75 GHz downconverted from the signal at the center frequency of the MMW signal of 92.5 GHz to the IF-band signal component at the center frequency of 17.5 GHz. Therefore, the main lobe component was not centered in the observed FFT spectra. For the 10-GBd signal, main lobe components with some sidelobes were fully captured by the ADC because the bandwidth of the main lobe component of the 10-GBd signal was 20 GHz, given that the ADC bandwidth was 30 GHz. However, for the 20-GBd signal, the main lobe component could not be fully acquired because of its bandwidth of 40 GHz. Generally, the modulated signal is comprised of symbol information and a pulse shape. For example, a rectangle pulse sequence has symbol information with a bandwidth of 10 GHz located at the center frequency and pulse shape information with an additional bandwidth of 10 GHz for a 10-GBd signal; thus, the total bandwidth is 20 GHz. From this perspective, the symbol information for the 20-GBd signal should be located at the center frequency with a bandwidth of 20 GHz; that is, the information should be at frequencies from 7.5 GHz to 27.5 GHz. Therefore, the symbol information could be captured and demodulated. We reported the successful demonstration of a high-baud-rate symbol using a narrow-bandwidth ADC [15], [20], whereby the symbol

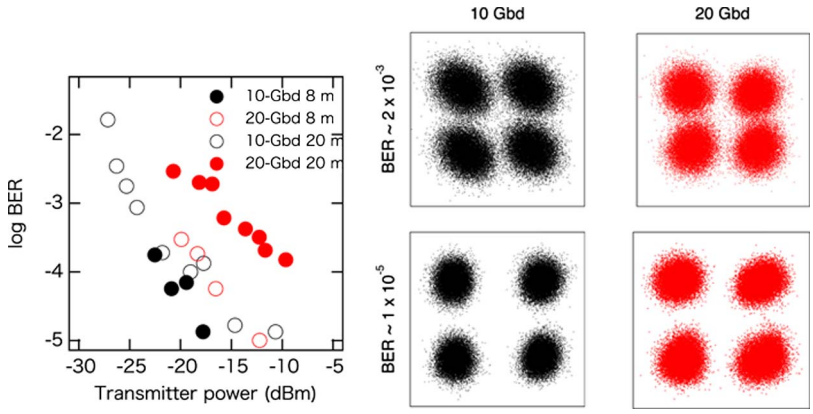

Fig. 6. Observed BERs for 10-GBd (black) and 20-GBd (red) signals under transmission distances of 8 m (open circles) and 20 m (solid circles) [15] (left). Observed constellation maps for 10-GBd and 20-GBd signals with BERs of 2×10^{-3} and 2×10^{-4}, respectively, under a 20-m transmission condition (right).

TABLE 1

Estimated achievable distance for 90-GHz radio transmission. Sensitivities are estimated from the transmitter power at a BER of 10^{-3} from Fig. 6

Radio output power	10 dBm	20 dBm	30 dBm
10 Gbaud (sens:−25 dBm)	450 m	1050 m	2040 m
20 Gbaud (sens: −15 dBm)	170 m	450 m	1050 m

information could be fully captured. There is no significant difference between different transmission distances. This indicates that the frequency-selective fading effect is not an issue under these conditions.

The observed BERs are shown in Fig. 6. All the BERs are within an FEC limit of a BER of 2×10^{-3}, and thus, the 10-GBd and 20-GBd QPSK transmissions were successfully performed with a total capacity of 18.6 Gb/s and 37.2 Gb/s, respectively, including a 7% FEC overhead [15]. The observed constellation maps of the QPSK signals are also shown in Fig. 6. Clear QPSK symbol separation without an IQ imbalance was observed for a BER of 10^{-5} as well as a BER near the FEC limit. This indicates that the direct photonic upconversion, depending on the incident optical power, cannot affect the radio signal quality, and thus, the linearity of the O/E conversion of the UTC-PD was maintained under this optical launch power condition. Under 8-m transmission through the air, the power penalty between 10-GBd and 20-GBd transmissions was estimated to be about 3 dB, and the power penalty for 20-m transmission was about 10 dB. This difference in penalties might be caused by the bandwidth issue of the ADC for the signal described in earlier text and the transmission distance [20]. In fact, the results for 8-m transmissions seem to show similar behavior, although the 20-GBd transmissions show some dependence on transmission distance. Here, the Fraunhofer distance of $2D^2/\lambda$ (where D and λ indicate the diameter of the antenna and the wavelength of the radio signal, respectively), which marks the traditional boundary between the near-field and far-field, was approximately 250 m, and thus, these experiments were performed under near-field conditions. A difference between the power penalties may exist because the received radio power significantly depends on the distance between the Tx and the Rx.

For application to an access network, the achievable distance is an important issue under this configuration. Table 1 summarizes and Fig. 7 shows the estimated achievable distance with various radio output powers. One should note that the sensitivity assumed for the transmitter power produced a BER of 10^{-3} for signals with each symbol rate, as shown in Fig. 6. The propagation loss

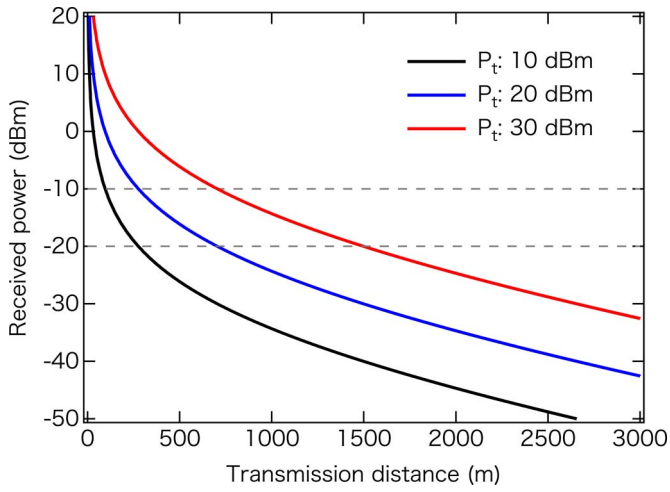

Fig. 7. Estimated achievable distance of 90-GHz radio transmission for transmitter powers of 10 dBm (black), 20 dBm (blue), and 30 dBm (red). Sensitivities (dashed gray lines) are estimated from the transmitter power at a BER of 10^{-3} from Fig. 6.

was calculated with the Friis transmission equation, considering a free-space propagating loss model, and the atmospheric attenuation coefficient was set at 1 dB/km, which is slightly larger than the reported value [21]. In this high-attenuation situation, propagation loss is mainly caused by atmospheric attenuation. When the radio output power is 10 dBm, the estimated transmission distance is less than 500 m for each symbol rate. An output power of more than 10 dBm can be realized using a commercially available power amplifier. With a power of up to 30 dBm, which can be realized by using a power combination technique and semiconductor-based power amplifiers, the transmission distance of 10-GBd QPSK communication can be extended to 1000 m [13]. This distance is applicable to midrange FWA transmission, such as building-to-building communication. For larger distances, an amplifier with an output power higher than 30 dBm is indispensable. When the power is under 30 dBm, the estimated transmission distance for 10-GBd QPSK as well as 20-GBd QPSK is 1000 m. A high-power amplifier based on GaN with an output power of 30 dBm has already been reported, and thus, its application to an access network would be feasible. Recently, a 40-dBm power amplifier based on vacuum-tube electronics has been also reported [14]. An extension of the transmission distance to longer than 3 km would be possible using these recently reported devices. However, such high-power devices have a limited available bandwidth, which is typically 5% to 7% of the carrier frequency. To enhance the throughput and distance, higher-order multilevel modulation, such as 16-ary quadrature amplitude modulation, and multicarrier modulation such as orthogonal frequency-division multiplexing (OFDM) will be an indispensable feature [8]. Phase noise tolerance might be an important issue under such long-distance transmission. Insertion of pilot tones in the signal, which method is similar to the OFDM technique, will suppress the phase noise effectively even in a single-carrier modulation [22].

5. Conclusion

We proposed an optical and radio seamless conversion network using a coherent RoF technique. A reduction in the number of DSPs at the RAU reduced the energy consumption and latency of the transmission system. High-speed RoF and its transmission with high-gain antennas were demonstrated as the proof of concept. The achieved data rate was 37.2 Gb/s for a 20-GBd QPSK signal with a 7% FEC overhead. When a high-power amplifier with an output power higher than 20 dBm was utilized, the transmission distance was extended to 2 km under 10-GBd operation. Seamlessly connected RoF optical and MMW radio transmission should be feasible for mobile backhauling, last-mile broadband access networks, and resilient access networks.

Acknowledgment

The authors would like to thank Dr. K. Fujii and Dr. T. Tosaka of the Applied Electromagnetic Research Institute at the National Institute of Information and Communications Technology, Japan, for help with using the large-scale anechoic chamber.

References

[1] I. Sugino, "Disaster recovery and the R&D policy in Japan's telecommunication," in *Proc. Opt. Fiber Conf.*, Los Angeles, CA, 2012.
[2] *The NTT Group's Response to the Great East Japan Earthquake*, NTT Group, Tokyo, Japan, CSR Rep. 2011, Dec. 2011.
[3] C. H. Schultz, K. L. Koenig, and E. K. Noji, "A medical disaster response to reduce immediate mortality after an earthquake," *New Engl. J. Med.*, vol. 334, no. 7, pp. 438–444, Feb. 1996.
[4] ITU-R WP5D. [Online]. Available: http://www.itu.int/ITU-R/
[5] IEEE802 LAN/WAN Standards Committee. [Online]. Available: http://www.ieee802.org/
[6] M. Weiss, A. Stöhr, F. Lecoche, and B. Charbonnier, "27 Gbit/s photonic wireless 60 GHz transmission system using 16-QAM OFDM," in *Proc. IEEE Int. Topic. Meeting MWP*, Valencia, Spain, postdeadline, Oct. 2009, pp. 1–3.
[7] X. Pang, A. Caballero, A. Dogadaev, V. Arlunno, R. Borkowski, J. S. Pedersen, L. Deng, F. Karinou, F. Roubeau, D. Zibar, X. Yu, and I. T. Monroy, "100 Gbit/s hybrid optical fiber-wireless link in the W-band (75–110 GHz)," *Opt. Exp.*, vol. 19, no. 25, pp. 24 994–24 949, Dec. 2011.
[8] A. Kanno, K. Inagaki, I. Morohashi, T. Sakamoto, T. Kuri, I. Hosako, T. Kawanishi, Y. Yoshida, and K. Kitayama, "40 Gb/s W-band (75–110 GHz) 16-QAM radio-over-fiber signal generation and its wireless transmission," *Opt. Exp.*, vol. 19, no. 26, pp. B56–B63, Dec. 2011.
[9] A. Kanno, T. Kuri, I. Hosako, T. Kawanishi, Y. Yasumura, Y. Yoshida, and K. Kitayama, "Coherent wired/wireless seamless transmission with combination of photonic digital and analogue techniques," in *Proc. IEEE Photon. Conf.*, Burlingame, CA, 2012, WAA1.
[10] T. Kuri, Y. Omiya, T. Kawanishi, S. Hara, and K. Kitayama, "Optical transmitter and receiver of 24-GHz ultra-wideband signal by direct photonic conversion techniques," in *Proc. IEEE Int. Topic. Meeting MWP*, Grenoble, France, Oct. 2006, pp. 1–4.
[11] R. Sambaraju, D. Zibar, A. Caballero, I. T. Monroy, R. Alemany, and J. Herrera, "100-GHz wireless-over-fiber links with up to 16-Gb/s QPSK modulation using optical heterodyne generation and digital coherent detection," *IEEE Photon. Technol. Lett.*, vol. 22, no. 22, pp. 1650–1652, Nov. 2010.
[12] A. Kanno, T. Kuri, I. Hosako, T. Kawanishi, Y. Yoshida, Y. Yasumura, and K. Kitayama, "High-speed fiber-optic and wireless transmission with RoF and digital coherent communication technologies," in *Proc. Asia-Pac. Microw. Photon. Conf.*, Kyoto, Japan, 2012, Th.B-3.
[13] M. Micovic, A. Kurdoghlian, A. Margomenos, D. F. Brown, K. Shinohara, S. Burnham, I. Milosavljevic, R. Bowen, A. J. Williams, P. Hashimoto, R. Grabar, C. Butler, A. Schmitz, P. J. Willadsen, and D. H. Chow, "92–96 GHz GaN power amplifiers," in *Pro. IEEE Int. Microw. Symp. Tech. Dig.*, Montreal, QC, Canada, Jun. 2012, pp. 1–3.
[14] Y. Hu, J. Feng, J. Cai, Y. Du, Y. Tang, X. Wu, Y. Chen, and W. Gao, "Development of W-band CW TWT amplifier," in *Proc. IEEE Int. Vac. Electron. Conf. Tech. Dig.*, Monterey, CA, Apr. 2012, pp. 295–296.
[15] A. Kanno, P. T. Dat, T. Kuri, I. Hosako, T. Kawanishi, Y. Yoshida, Y. Yasumura, and K. Kitayama, "20-Gbaud QPSK optical and radio transmission using high-gain antennas for resilient access networks," in *Proc. IEEE Photon. Soc. Summer Topic. Meeting Opt. Wireless Syst. Appl.*, Seattle, WA, 2012, pp. 145–146.
[16] A. Kanno, K. Inagaki, I. Morohashi, T. Kuri, I. Hosako, and T. Kawanishi, "Frequency-stabilized W-band two-tone optical signal generation for high-speed RoF and radio transmission," in *Proc. IEEE IPC*, Arlington, VA, Oct. 2011, pp. 272–273.
[17] T. Kawanishi, T. Sakamoto, and M. Izutsu, "High-speed control of lightwave amplitude, phase, and frequency by use of electrooptic effect," *IEEE J. Sel. Topics Quantum Electron.*, vol. 13, no. 1, pp. 79–91, Jan./Feb. 2007.
[18] H. Kiuchi, T. Kawanishi, M. Yamada, T. Sakamoto, M. Tsuchiya, J. Amagai, and M. Izutsu, "High extinction ratio Mach–Zehnder modulator applied to highly stable optical signal generator," *IEEE Trans. Microw. Theory Tech.*, vol. 55, no. 9, pp. 1964–1972, Sep. 2007.
[19] R. Yamanaka, T. Fujita, H. Sotobayashi, A. Kanno, and T. Kawanishi, "Analysis of phase noise of frequency quadrupler using dual-drive Mach–Zehnder modulator and two free running lasers," in *Proc. Asia-Pac. Microw. Photon. Conf.*, Kyoto, Japan, 2012, PA-6.
[20] A. Kanno, T. Kuri, I. Hosako, T. Kawanishi, Y. Yasumura, Y. Yoshida, and K. Kitayama, "20-Gbaud QPSK RoF and millimeter-wave radio transmission," in *Proc. 17th OptoElectron. Commun. Conf.*, Busan, Korea, 2012, pp. 735–736.
[21] *Attenuation of Atmospheric Gases*, ITU, Geneve, Switzerland, Rec. ITU-R P.676-5, 2001.
[22] W. Shieh, H. Bao, and Y. Tang, "Coherent optical OFDM: Theory and design," *Opt. Exp.*, vol. 16, no. 2, pp. 841–859, Jan. 2008.